

Comparison of Shear-Thinning Blood Flow Characteristics between Longitudinal and Transverse Vibration

Sung-Ho Choi, Sehyun Shin*

*School of Mechanical Engineering, Kyungpook National University,
1370 Sangyeok-dong, Buk-gu, Daegu 702-701, Korea*

Kyung-Tae Lee

*Department of Aerospace Engineering, Sejong University,
98 Gunja-Dong, Gwangjin-Gu, Seoul 143-747, Korea*

This article described the numerical investigation of shear-thinning blood flow characteristics when subjected to longitudinal and transverse vibrations and delineated the underlying mechanisms of the flow rate enhancements, respectively. In order to fully consider the mechanical vibrations of the capillary, a moving wall boundary condition was adopted. The present numerical results showed that the longitudinal vibration caused a significant increase of wall shear rates, which resulted in a decrease of viscosity and the subsequent increase of flow rates. However, the shear rate for the transverse vibration was slightly increased and the calculated flow rate was underestimated comparing with the previous experimental results.

Key Words : Shear-Thinning, Vibration, Flow Rate, Vibration-Induced Shear, Viscosity

Nomenclature

D : Diameter (m)
 f : Vibration frequency (Hz)
 g : Gravitational acceleration (m/s^2)
 L : Length (m)
 n : Power law index
 p : Pressure (Pa)
 t : Time (s)
 Q : Volume flow rate (m^3/s)
 v : Velocity (m/s)

λ : Time constant in Carreau model (s)
 ω : Angular frequency (s^{-1})

Subscripts

i : Initial
 θ : Component in peripheral direction
 r : Component in radial direction
 w : Wall
 z : Component in axial direction

Greek Symbols

Δ : Vibration amplitude (m)
 ρ : Density (kg/m^3)
 γ : Shear rate (s^{-1})
 η : Non-Newtonian viscosity ($Pa \cdot s$)
 η_0 : Zero shear rate viscosity ($Pa \cdot s$)
 η_∞ : Infinite shear rate viscosity ($Pa \cdot s$)

1. Introduction

Understanding non-Newtonian fluid flows has become increasingly important in many industrial applications, including the processing of polymers, foams, pharmaceuticals, personal care products, and blood circulation. When one deals with a practical engineering problem consisting of a non-Newtonian fluid, however, it is not easy to estimate the flow rate in a simple condition such as an oscillating circular pipe. The reason is that the flow rate of non-Newtonian liquids varies according to shear rates, a phenomenon that is strongly affected by rheological

* Corresponding Author,

E-mail : shins@wmail.knu.ac.kr

TEL : +82-53-950-6570; FAX : +82-53-956-9914

School of Mechanical Engineering, Kyungpook National University, 1370 Sangyeok-dong, Buk-gu, Daegu 702-701, Korea. (Manuscript Received December 8, 2003; Revised September 30, 2004)

properties. Consequently, the velocity and shear fields differ from those obtained with a constant-property fluid, whose viscosity is independent of shear rate.

There are many research reports concerning the flow behaviour of non-Newtonian fluids that are subjected to a mechanical vibration or oscillation. It has been reported that mechanical vibrations causes flow enhancement for shear-thinning fluids, whereas they cause flow retardation for shear-thickening fluids (Phan-Thien and Dudek, 1982). The "shear-thinning" fluid is defined as a fluid which viscosity decreases with increasing shear rate. Typical shear-thinning fluids are blood, polymeric solutions, dairy food, and various suspensions.

There was an interesting research report regarding non-Newtonian viscosity with the longitudinal vibration. Deshpande and Barigou (2001) investigated the effects of vibrations on flow characteristics and reported that the flow enhancement was observed for a shear-thinning fluid by applying the longitudinal vibration to a flowing tube. In addition, the flow enhancement was a function of both the vibration frequency and amplitude. A shear-independent fluid such as water showed no difference whether vibrations were applied or not. Prior to this report, in fact, there were several reports on the flow of non-Newtonian fluids in a pipe under the influence of the longitudinal vibration (Goshawk et al., 1994; Deysarkar et al., 1981). These studies reported the enhancement of a flow rate when a non-Newtonian fluid that flows through a pipe is subjected to the longitudinal vibration.

Recently, Shin et al. (2003a; 2003b) investigated the effect of a transverse vibration on the flow characteristics of blood and RBC suspensions. In fact, blood is a typical shear-thinning fluid. They reported that the blood flow resistance was strongly dependent upon both the vibration frequency and amplitude. In addition, Suh et al. (1998) studied the effects of vibrations on blood viscosity and reported that blood viscosity diminished as much as 10–12% by applying the transverse vibration. It, however, is not clear whether these experimental results were caused by

the vibration-induced shear increase or not. For transversal vibration, there has not been a comprehensive study to delineate the mechanism of flow rate enhancement when a shear-thinning blood flow is subjected to transversal vibrations. Furthermore, there has not been a study to compare flow characteristics under both longitudinal and transversal vibration. Therefore, the objective of the present study is to investigate the flow structure of a shear-thinning fluid when it is subjected to longitudinal and transverse vibrations, respectively and to understand the underlying mechanism of the flow rate enhancement associated with each vibration.

2. Numerical Analysis

The present study conducted numerical analyses for the flow with a longitudinal and transverse vibration. It was assumed that the flow through a capillary was laminar, incompressible, and isothermal. The vibration subjected to the capillary tube was a sinusoidal function and the directions of the vibration are longitudinal and transverse to the flow direction. It is worthy to note that the tube flow with the transverse vibration is not axisymmetric, which requires a fully three-dimensional flow analysis.

The governing equations include the equations of continuity and motion as follows :

$$\nabla v = 0 \quad (1)$$

$$\rho \frac{Dv}{dt} = -\nabla p + [\nabla \eta \dot{\gamma}] + \rho g \quad (2)$$

where v is fluid velocity, p is fluid pressure, t is time, η is the apparent viscosity, ρ is fluid density, and g is the gravitational acceleration. In addition, the apparent viscosity for blood, which is the same test fluid in the previous experiment (Shin et al., 2003a), was described by adopting the Carreau model :

$$\eta = \eta_{\infty} + (\eta_0 - \eta_{\infty}) [1 + (\lambda \dot{\gamma})^2]^{(n-1)/2} \quad (3)$$

where η_0 is the zero shear rate viscosity (0.065 Pa·s), η_{∞} is the infinite shear rate viscosity (0.004 Pa·s), n is the power law index (0.65) and λ is the characteristic time constant (17 s).

Figure 1 shows a three-dimensional computational model of the present study. To simulate the previous experiment (Shin et al., 2003a), constant pressure conditions were given at inlet and outlet, respectively. In order to fully consider the mechanical vibration of the capillary, a moving wall boundary condition was adopted. For the vibrations subjected to the capillary tube, a sinusoidal vibration on the wall was applied in the longitudinal and transverse directions of the flow, respectively, as shown in Eq. (4) and Eq. (5)

$$z = A \sin(\omega t) \text{ for longitudinal vibration} \quad (4)$$

$$r = A \sin(\omega t) \text{ for transverse vibration} \quad (5)$$

where $\omega (=2\pi f)$ is the angular frequency of vibration. Then, the boundary conditions of the longitudinal and transverse vibrations at the wall ($r=R$) become Eqs. (6) and (7), respectively.

$$\begin{aligned} v_z(R, \theta, z) = A\omega \cos(\omega t), v_r(R, \theta, z) = 0 \\ v_\theta(R, \theta, z) = 0 \end{aligned} \text{ for longitudinal vibration} \quad (6)$$

$$\begin{aligned} v_z(R, \theta, z) = 0, v_r(R, \theta, z) = A\omega \cos(\omega t) \\ v_\theta(R, \theta, z) = 0 \end{aligned} \text{ for transverse vibration} \quad (7)$$

The boundary conditions in Eqs. (6) and (7) reflect a condition of no slip at the wall, which were applied for both the steady and unsteady flow.

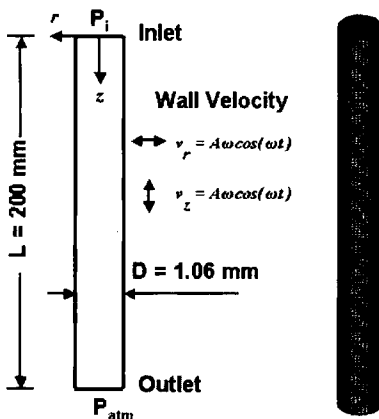


Fig. 1 A three-dimensional computational model and schematic diagram

A numerical analysis was conducted in two steps: First, a steady-state flow through a capillary was solved without vibration. Then, using the converged steady-state velocity field, an unsteady flow analysis was conducted considering the effect of vibrations with respect to time. In order to fully appreciate the effect of the vibrations, there were a sufficient number of grids ($20 \times 20 \times 100$), (R, θ, z) and 200 time steps during the 6 periods of the sine wave for the numerical modelling. At each time step, the corresponding flow rate was calculated. The present study adopted a commercial CFD code, CFD-ACE (CFDRC, 2003) as a numerical analysis tool.

3. Results and Discussion

Figure 2 shows the normalized flow rates versus vibration frequency comparing longitudinal vibrations with a transverse one for a shear-thinning fluid. As the vibration frequency increases, the flow rate for the longitudinal vibration significantly increases. These results for the longitudinal vibrations are in good agreement with the previous study (Deshpande and Barigou, 2001). The flow rate for the transverse vibration, however, slightly increases (10%) with the fre-

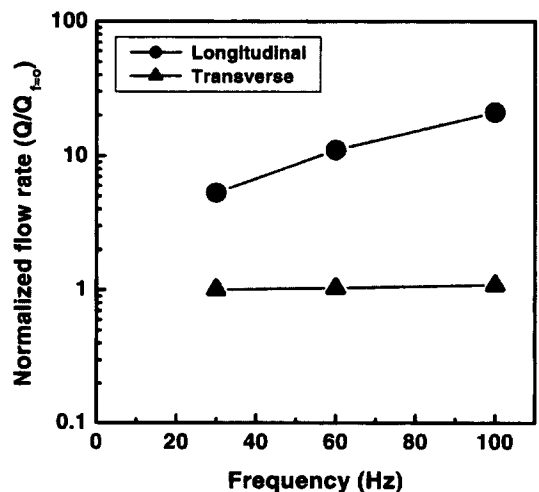


Fig. 2 Normalized flow rate for various frequencies for longitudinal and transverse vibrations at a fixed amplitude ($\Delta=0.3$ mm)

quency. It is worthy to note that while the vibration frequency varies, the vibration amplitude is fixed at $\Delta=0.3$ mm.

Figure 3 shows the normalized flow rate versus vibration amplitude, which compares the longitudinal vibration with a transverse one for a shear-thinning fluid. The results are very similar to those in Fig. 2. As the vibration amplitude increases, the flow rate for the longitudinal vi-

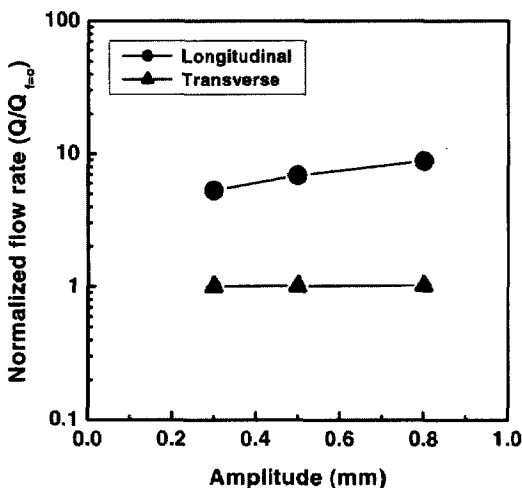


Fig. 3 Normalized flow rate for various amplitudes for longitudinal and transverse vibrations at a fixed frequency ($f=30$ Hz)

bration significantly increases, whereas that for transverse vibration slightly increases. In this case, the vibration frequency remained constant as $f=30$ Hz.

Comparing the flow rates between these phenomena, there should be apparently different mechanisms governing the flow characteristics, respectively. Thus, there is a need to look inside the flow structure to discover the governing mechanisms for these phenomena. Figure 4 shows the transient characteristics of a flow rate and pressure with respect to time for the longitudinal and transverse vibrations. As shown in Fig. 4(a), the flow rate for the longitudinal vibration shows a sinusoidal curve having a phase lag of 0.18π compared with the wall velocity. Meanwhile, the flow rate-time curve for the transverse vibration is almost flat and shows a phase lag of 0.59π compared with the wall velocity. Figure 4(b) shows the transient characteristics of the wall pressure with respect to time. The wall pressure data was obtained at $z/L=0.5$ for transverse vibration and $r/R=1$ for longitudinal vibration, respectively. As shown in Fig. 4(b), the wall pressure for the longitudinal vibration does not vary significantly. In case of the transverse vibration, however, the wall pressure significantly fluctuates in a sinusoidal function having a phase

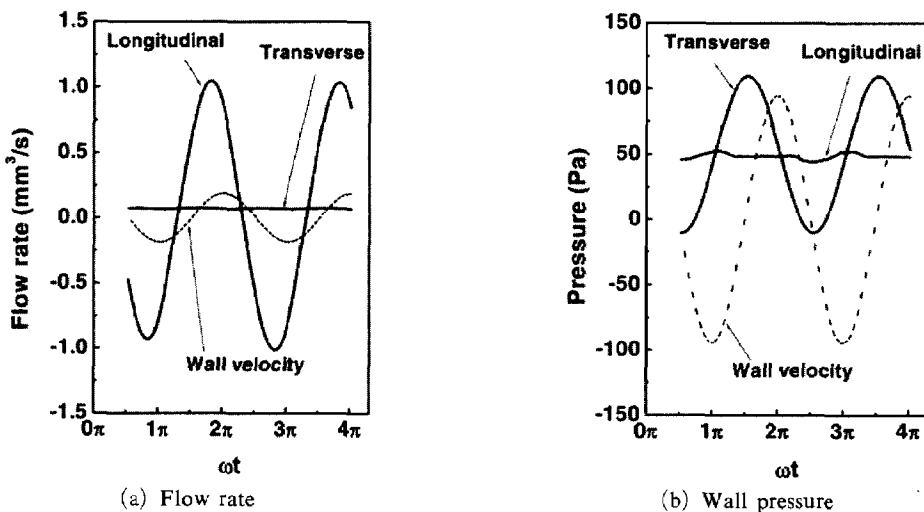


Fig. 4 Transient characteristics for longitudinal and transverse vibrations. The wall pressure was obtained at $z/L=0.5$ for transverse vibration and $r/R=1$ for longitudinal vibration, respectively

lag of $\pi/2$.

Figure 5 compares the velocity profiles between the longitudinal and transverse vibrations at $z/L=0.5$. Prior to explaining the figures, it may be useful to recall that $\omega t=2n\pi$ and $2n\pi+\pi$ indicate when the displacement is zero and the wall velocity is maximum and $\omega t=2n\pi+\pi/2$ and $2n\pi+3\pi/2$ indicate when the displacement

is maximum and the wall velocity is zero. Fig. 5 (a) shows the velocity profiles for the transverse vibration, which does not show a significant change with the vibration ($f=100$ Hz). On the other hand, for the longitudinal vibrations, the velocity profile significantly changes with time. Owing to the no-slip condition with vibrated wall, the flow near the wall moves at the same velocity of the wall. At $\omega t=2n\pi+\pi$ and $2n\pi+3\pi/2$, the velocity profiles show negative values (i.e., backflow occurs) and at $\omega t=2n\pi$ and $2n\pi+\pi/2$, positive. It is worthy to note that the maximum velocity for the longitudinal vibration ($f=100$ Hz, $\Delta=0.3$ mm) is almost 750 times larger than that for the no-vibration, as shown in Fig. 5. This result implies that there is a significant increase in the shear rate which is associated with the velocity gradient.

Figure 6 shows a comparison of the pressure profiles between the longitudinal and transverse vibrations. For the transverse vibration, the pressure profile at $z/L=0.5$ drastically varies with time as shown in Fig. 6(a). When the displacement is maximum ($\omega t=2n\pi+\pi/2$ and $2\pi+3\pi/2$), the pressure profiles show steep gradients in the radial direction. Even for the high radial pressure gradient, however, there is no flow in the radial direction and these radial pressure gradients do not affect the main flow as shown

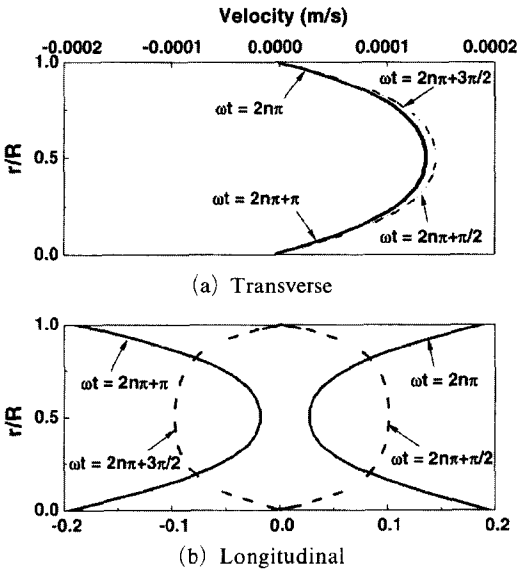


Fig. 5 Comparison of the velocity profiles between longitudinal and transverse vibrations at $z/L=0.5$

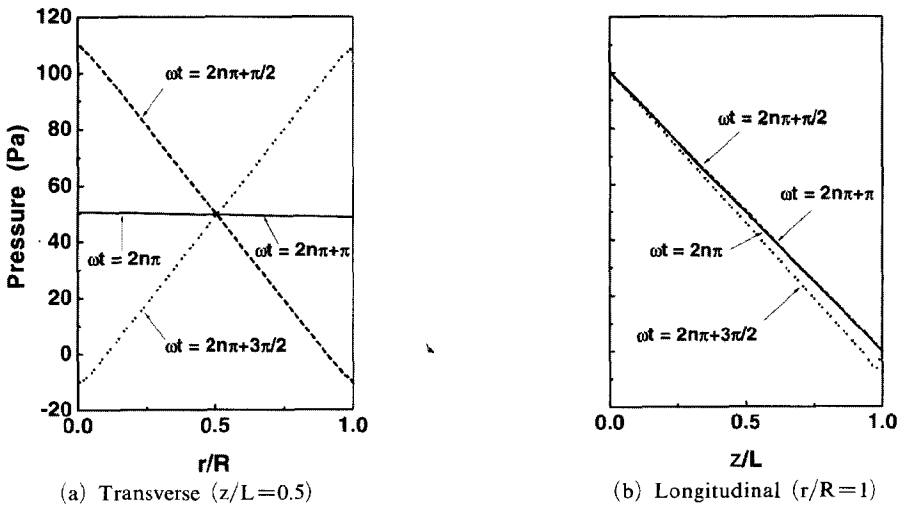


Fig. 6 Comparison of the pressure profiles between longitudinal and transverse vibrations

in Fig. 5(a). Thus, the flow with transverse vibrations is mainly driven by the pressure difference between the inlet and outlet. Meanwhile, the pressure profiles for the longitudinal vibrations do not vary much with time as shown in Fig. 6(b). Thus, the flow with the longitudinal vibrations is a combination of a pressure-driven flow and vibration-induced drag flow.

Figure 7 shows the relative wall shear rate versus the vibration shear rate for longitudinal and transverse vibrations. The relative wall shear rate is a ratio of the wall shear rate with vibrations to that without vibration ($\dot{\gamma}_w/\dot{\gamma}_{w,f=0}$), whereas the vibration shear rate is defined as a product of the frequency and amplitude of vibrations divided by a characteristic length ($f\Delta/D$). In Fig. 7, the longitudinal vibrations cause a significant increase in the shear rate, whereas the transverse vibration causes a slight increase in the shear rate. For longitudinal case, the data shows slightly meandering trend, which may be due to the numerical error associated with modelling of non-Newtonian viscosity. However, this meandering data is acceptable since it shows apparently the strong correlation between the shear rate and vibration. This result implies that the significant increase in the shear rate may reduce the viscosity for shear-thinning fluids, which subsequently results in an increase of the

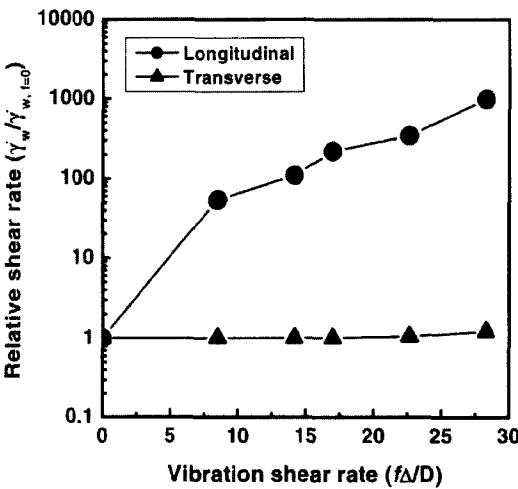


Fig. 7 Relative wall shear rate vs. vibration shear rate for longitudinal and transverse vibrations

flow rate.

Figure 8 shows comparison of the present numerical results with the previous experiments. In this comparison, the present numerical results showed good agreement with the experimental result at high flow rate. At low flow rate, however, there was a significant difference between them. These results imply that the vibration effect is dominant in low-shear flow conditions. However, the numerical analysis cannot predict the flow rate increase with vibration in the experiment.

From the results shown in Figs. 7 and 8, the shear increase due to the transverse vibration is negligibly small that its corresponding shear-thinning effect does not play a significant role on the flow rate enhancements. Thus, the present study cautiously concludes that the vibration-induced shear increase is not the main parameter causing the flow rate enhancement with transverse vibration. With excluding the effect of vibration-induced extra shear on flow rate enhancement, the other possible candidate mechanism is a vibration-induced rheological property change. In fact, the previous experimental results (Shin et al., 2003a) showed decrease of flow resistance with increasing transverse vibration intensity. In addition, they found the re-

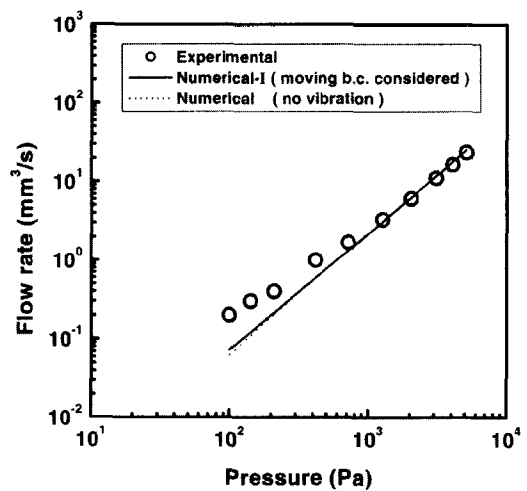


Fig. 8 Comparison of flow rate along driving pressure for both experimental and numerical analysis ($f=100$ Hz, $A=0.3$ mm)

versible change of viscosity when vibration is removed. However, it is not clear that transverse vibration may induce viscosity reduction for non-Newtonian fluid such as aqueous polymer solution and blood.

Conclusively, the mechanism for the flow rate enhancement for shear-thinning blood flow is mainly interpreted by an extra shear rate increase due to vibrations in the present numerical study. The vibrations, however, may cause not only an extra increase in the shear rate but also changes in the internal structure of materials and rheological properties of non-Newtonian fluids. Thus, further study should consider rheological change that is associated with material structure as well as an extra increase in the shear rate due to vibrations.

4. Conclusion

The present study numerically investigated the flow structures for shear-thinning fluid with longitudinal and transverse vibrations and delineated the underlying mechanism of the flow rate enhancement. The longitudinal vibrations caused a significant increase in the shear rate near the wall, which resulted in a reduction of apparent viscosity and a subsequent increase in the flow rate for shear-thinning fluids. The transverse vibrations, however, caused slight increase of shear rate and little decrease of viscosity, which resulted in slight increase of flow rate. The present study confirmed that the vibration induced shear rate increase played an important role in the drag reduction for shear-thinning fluid such as blood and RBC suspensions.

Acknowledgment

This work was supported by a grant from the National Research Laboratory of the Ministry of Science and Technology, Korea. The authors wish to express their appreciation for the support.

References

- CFDRC., 2003, "CFD-ACE Manual," Huntsville., USA.
- Deshpande, N. S. and Barig, M., 2001, "Vibrational flow of Non-Newtonian fluids," *Chem. Eng. Sci.*, Vol. 56, pp. 3845~3853.
- Deysarkar, A. K. and Turner, G. A., 1981, "Flow of Paste in a Vibrated Tube," *J. Rheology*, Vol. 25, pp. 41~54.
- Goshawk, J. A. and Walters, K., 1994, "The Effect of Oscillation on the Drainage of an Elastic-Viscous Liquid," *J. Non-Newtonian Fluid Mech.*, Vol. 54, pp44p.
- Phan-Thien, N. and Dudek, J., 1982, "Pulsating Flow Revisited," *J. Non-Newtonian Fluid Mech.*, Vol. 11 pp. 147~161.
- Suh, S., Yoo, S., Kim, D. I. and Lee, B., 1998, "Effect of Physical Vibration in Blood Viscosity," *J. Korean Vascular Surgery Society.*, Vol. 14, No. 1, pp. 29~32.
- Shin, S., Ku, Y. H., Moon, S. Y. and Suh, J. S., 2003a, "Vibration on the Hemorheological Characteristics of Non-Aggregated Blood," *KSME Int. J.*, Vol. 17, pp. 1104~1110.
- Shin, S. and Lee, J. H., 2003b, "Characteristics of Shear-Thinning Fluid Viscosity Under Traversal Vibration in a Circular Capillary Flow," *Jap. J. Applied Physics.*, Vol. 78, pp. 256~272.